Chemical Engineering Journal 142 (2008) 285–300

Contents lists available at ScienceDirect

Chemical Engineering Journal

journal homepage: www.elsevier.com/locate/cej

Optimization of primary enrichment section of mono-thermal ammonia–hydrogen chemical exchange process

M.R. Sawant [a], K.V. Patwardhan [a], A.W. Patwardhan [a], V.G. Gaikar [a,*], M. Bhaskaran [b]

[a] Institute of Chemical Technology, University of Mumbai, Matunga, Mumbai 400019, India
[b] Heavy Water Board, V. S. Bhavan, Anushakti Nagar, Mumbai 400094, India

ARTICLE INFO

Article history:
Received 18 August 2007
Received in revised form 14 February 2008
Accepted 25 February 2008

Keywords:
Absorption
Chemical exchange
Deuterium
Separations
Rate based model
PIEU

ABSTRACT

A comprehensive model of Primary Enrichment Section (PES) comprising of preliminary isotopic exchange unit (PIEU), ammonia synthesis unit, catalyst stripping unit, ammonia cracker and heat exchange network (HEN) has been developed to determine optimized conditions for heavy water production. A separate PIEU simulation carried out in the previous work has predicted a high temperature operation would be beneficial for the increased deuterium extraction [M.R. Sawant, A.W. Patwardhan, V.G. Gaikar, Simulation of the mono-thermal ammonia hydrogen chemical exchange tower as reactive absorption system, Ind. Eng. Chem. Res. 45 (20) (2006) 6745]. However, it would be limited by adverse effect of the increased temperature on the ammonia synthesis unit. The entire Primary Enrichment Section (PES) is, therefore, simulated to quantify the effect of the operating variables on the throughput of NH_2D from this section. The model predicts that, by increasing the operating temperature of the PES from 248 K to 258 K would not only reduce the energy requirement in the HEN by 50% but also increases the productivity of heavy water by 7%.

1. Introduction

The chemical exchange processes dominate the production of heavy water world over accounting to more than 95% of the total production of heavy water [1]. In large scale set-ups of heavy water production, the chemical exchange is used for primary enrichment of deuterium up to 10–25%, followed by either distillation or electrolysis for the final enrichment to nuclear grade heavy water (99.8%) [1].

The chemical exchange involves an isotopic exchange reaction between two chemically distinct substances, resulting in isotopic redistribution between the exchanging species without altering their chemical nature. Thus, in the NH_3–H_2 chemical exchange process a shift in the H/D ratio takes place when liquid ammonia is contacted with gaseous hydrogen in a counter-current manner by the following reaction

$$NH_{3(l)} + HD_{(g)} \Leftrightarrow NH_2D_{(l)} + H_{2(g)} \quad (1)$$

Potassium metal dissolved in liquid ammonia is used as a catalyst for this process. Two variations of the NH_3–H_2 chemical exchange process exist depending upon the method employed for providing reflux, viz. mono-thermal exchange process and Bi-thermal exchange process [1]. In the mono-thermal exchange process the reflux is obtained by chemical conversion whereas in the bi-thermal process the reversibility of the exchange reaction is exploited. The chemical exchange process requires a large amount of ammonia and hydrogen, thus the synthesis gas ($N_2 + 3H_2$) from a fertilizer plant is usually utilized in the process. A block diagram of the mono-thermal chemical exchange process is shown in Fig. 1. The Primary Enrichment Section (PES) (highlighted in Fig. 1) of the mono-thermal process consists of the preliminary isotopic exchange unit (PIEU) (comprising of the exchange towers, T1 and T2), heat exchange network (HEN) between T1 and T2, catalyst stripping unit (CSU), an ammonia converter and an ammonia cracker unit.

The feed syngas is compressed to a pressure which compensates the pressure drop due to routing of the gas through the chemical exchange plant before returning to the fertilizer plant [2]. The compressed gas is dried and purified to remove oxygenated impurities which otherwise can react with potassium amide and give rise to insoluble products which tend to clog the contact equipment [2]. The dried, purified and cooled synthesis gas then enters at the bottom of the first exchange tower T1 of the PIEU where it is contacted with counter flowing liquid ammonia containing potassium amide as the catalyst. The exchange tower T1 is typically operated in the range of 243–263 K and 18–25 MPa (Fig. 2). The deuterium from the

* Corresponding author. Fax: +91 22 24145614.
E-mail address: v.g.gaikar@udct.org (V.G. Gaikar).

1385-8947/$ – see front matter © 2008 Elsevier B.V. All rights reserved.
doi:10.1016/j.cej.2008.02.022

Nomenclature

a	activity of chemical species
C_p	heat capacity at constant pressure (J/mol K *unless specified*)
C_V	heat capacity at constant volume (J/mol K *unless specified*)
d	diameter (m *unless specified*)
f	geometric shape factor
F	gas flow from bed
G	molar flow of gas
h	enthalpy content
$\hbar$	heat transfer coefficient
H	Henry's constant
Ht	total height of catalyst bed (m)
K	equilibrium constant
l	length (m)
L	molar flow of liquid
$\dot{m}$	mass velocity
P	pressure
q	quench fraction
r	rate of reaction per cubic-meter of catalyst bed per hour
t	thickness (m)
U	overall heat transfer coefficient (kcal/h m^2 °C)
UA	lumped heat transfer parameter for heat exchange equipment
W	mass flow
X	deuterium fraction in the liquid phase
y	gas phase mole fraction
z	distance from top of converter bed

Greek letters

β	G/L separation factor
γ	activity coefficient
ϑ	catalyst activity
λ	thermal conductivity
μ	viscosity
ξ	effectiveness factor for the solid catalyzed gas phase reaction
ρ	density
ϕ	fugacity coefficient
χ	fractional conversion
ψ	lumped reaction parameter for ammonia converter

Subscripts and Superscripts

a	ammonia
ann	annulus
AT	annulus top
b	catalyst bed
bas	catalyst basket
bed	catalyst bed
bot	bottom
cra	cracker
D	deuterium
e	ejector tube
eqm	reaction equilibrium
F	feed
g	vapor phase
i	chemical species
i	inside
ins	catalyst basket insulation
int	interchanger
l	liquid phase
lm	log mean
o	outside
p	catalyst particle
ph	phase equilibria
P	product
ris	central riser tube
RT	riser top
S	shell-side
sat	saturation
t	tray
tube	interchanger, cracker tube
T	tube-side
0	condition at entry

hydrogen content of the syngas is transferred to the liquid phase by the isotopic exchange reaction given by Eq. (1). The liquid leaving the deuterium extraction tower (T1) is heated and expanded in the heat exchange network between T1 and T2, since the exchange tower T2 is operated at a higher temperature 273–281 K and low pressure 9–12 MPa. This deuterium rich liquid is further enriched in the exchange tower T2 by contacting with cracked syngas, rich in deuterium coming from the cracker. Thus, the liquid stream finally leaving the tower T2 gets enriched in deuterium to about 200 times the inlet concentration of deuterium in the feed syngas. At the bottom of the enrichment tower T2 a small portion of the deuterium rich syngas is withdrawn for final concentration. The reflux at both the ends of the PIEU is obtained by the chemical inter-conversion between syngas ($N_2 + 3H_2$) and ammonia (NH_3) [2].

The extraction of deuterium from the fresh syngas stream takes place in the Primary Enrichment Section (PES) which is considered at the heart of the entire mono-thermal chemical exchange process. In our previous work [3], the PIEU of the mono-thermal chemical exchange process has been modeled and simulated to locate an optimum operating window with respect to process variables viz. temperature, pressure, catalyst concentration and gas load. The model predicted that a higher operating temperature of the exchange tower T1 increases the deuterium extraction from the fresh syngas stream [3]. However, a high temperature of operation of the tower T1 invariably results in higher concentrations of ammonia in the syngas mixture leaving T1 and entering the ammonia synthesis unit (ASU). The ammonia synthesis unit provides the liquid reflux to the exchange tower T1 by chemically converting syngas to ammonia (Eq. (2))

$$\frac{1}{2}N_2 + \frac{3}{2}H_2 \Leftrightarrow NH_3 \quad (2)$$

A higher content of the product (i.e. NH_3) in the feed to the ammonia converter directly affects the conversion efficiency of the ammonia synthesis unit, consequently decreasing the liquid NH_3 throughput. A reduced liquid reflux affects the tower L/G ratio in the chemical exchange section and also reduces the final throughput of NH_2D from the PIEU. On the other hand, a higher operating temperature of the exchange towers can reduce the refrigeration requirements in the HEN between exchange towers T1 and T2 and thus the cost of heavy water production.

In the present work, the mathematical model of the PIEU is analyzed including the Primary Enrichment Section to study the overall effect of the operating temperature, pressure and the catalyst concentration on the final throughput of NH_2D from the Primary Enrichment Section (PES) and possible energy benefits thereof.

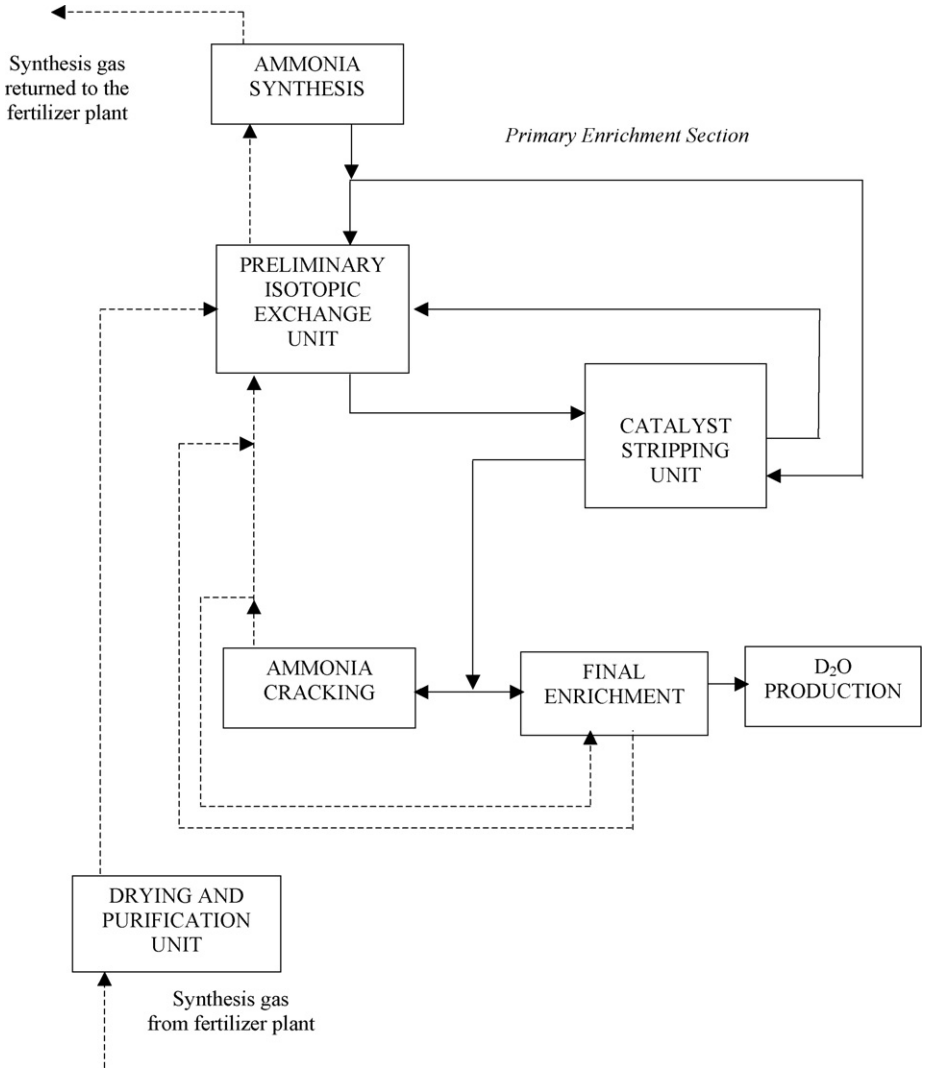

Fig. 1. The mono-thermal ammonia hydrogen chemical exchange process.

2. The heat exchange network (HEN) between T1 and T2

A detailed description of the preliminary isotopic exchange unit and the mathematical model to simulate the absorption of HD into liquid ammonia followed by the chemical exchange reaction has been provided elsewhere [3]. The exchange tower T1 is operated at a low temperatures and high pressures, principally to increase the solubility of HD and the performance of the ammonia synthesis unit, whereas tower T2 is operated at lower pressures and higher temperatures.

Since, the bulk liquid and gas streams of the two exchange towers are interconnected, a heat exchange network (HEN) has to be in place to achieve such significant variations in the operating conditions. The HEN between the exchange towers T1 and T2 as shown in Fig. 3 comprises of heat exchangers E1, E4 and E5, condensers R1 and R4 and humidification-cooling tower A11/A12.

The ammonia content in the synthesis gas ($N_2 + 3H_2$) leaving the exchange tower T2 depends on the temperature and pressure conditions of the tower. This synthesis gas, saturated with ammonia, is compressed to the operating pressure of tower T1 in the compressor K4. The gas gets heated, during the compression, to a higher temperature but retains the ammonia content of syngas same as that at the exit of tower T2. This superheated gas exchanges heat in a counter-current manner with the relatively cold liquid in heat exchanger E5. This gas is further condensed and cooled in the ammonia condenser R4; here liquid ammonia is used as refrigerant and is made available at a temperature in between those of operating temperatures of T1 and T2. This saturated two-phase flow from R4 is further routed through the heat exchanger E4 in a counter-current manner with the cold liquid leaving tower T1, where more ammonia is condensed. This two-phase mixture is then taken to vessel V4 where the gas and liquid streams are allowed to separate. The dried syngas stream ($N_2 + 3H_2$) from the fertilizer plant is cooled with the cold gas leaving tower T1 in the heat exchanger E1. This syngas stream is then combined with the saturated syngas stream from vessel V4 and cooled in condenser R1 (refrigerant ammonia at 248 K). The resultant unsaturated gas stream is sent to the humidification-cooling section A11/A12. Here, the unsaturated gas mixture is subjected to humidification-cooling and the temperature is brought down to the operating temperature of the tower T1. The ammonia required for humidification is taken from vessel V4.

The process side calculations for the heat transfer equipments in the HEN are performed to evaluate the heat transfer parameters. For a counter-flow type of heat exchanger, the energy balance equations based on the overall heat transfer coefficient U and the log mean

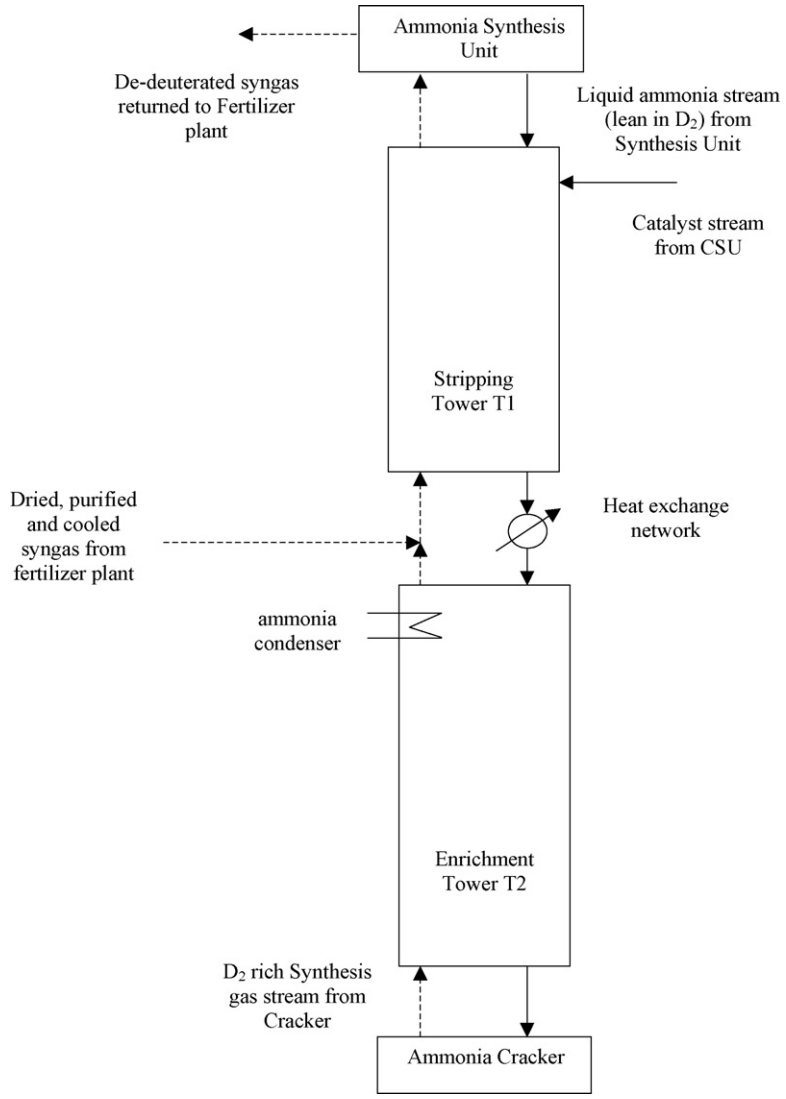

Fig. 2. The Preliminary Isotope Exchange Unit (PIEU) along with ammonia synthesis unit and cracker.

Table 1
The lumped parameter UA for heat transfer equipment in HEN

Heat exchange unit	UA (kcal/h °C)
E5	2250
R4	35629
E4	52000
R1	22819
E1	13751

temperature difference ΔT_{lm} are given as,

$$(UA)\Delta T_{lm} = \dot{m}_s C_p \Delta T_s = \dot{m}_T C_p \Delta T_T \quad (3)$$

The overall heat transfer coefficient U and the heat exchanger area A for the individual heat exchangers and condensers are lumped together as a single parameter UA and evaluated by utilizing the design data obtained from an existing heavy water plant for HEN. The corresponding values of the UA for the heat transfer equipments in the HEN are given in Table 1. These estimated design values of UA are utilized for the simulation of the Primary Enrichment Section (PES).

3. Catalyst separation and ammonia preparation for cracking

Fig. 4 shows the details of this section. The enriched liquid ammonia leaving T2 is heated in exchanger and expanded to about 2.5 MPa before entering vessel V1. Due to reduction in pressure four times, the dissolved synthesis gas in liquid ammonia coming from T2 is separated in V1. The liquid ammonia, to be fed to the cracker, should not contain any potassium amide as it fouls up the catalyst. The limit set for K^+ in ammonia is less than 0.1 ppm. The liquid should also be degassed as far as possible, to achieve maximum cracking efficiency. The liquid ammonia containing potassium amide flows by gravity to the steam heater H1 where it is vaporized. The vaporized ammonia and the concentrated amide solution get separated in C11. H1 and C11 work on a thermo-siphon principle. The necessary heat is provided by the low pressure saturated steam. The ammonia vapors from C11 enter the bottom portion of the column C1 and the entrained liquid is separated out.

The distillation column C1 consists of a total of 14 trays distributed over two sections: an upper part containing eight sieve trays to degas the ammonia and a lower part, containing six sieve trays to wash the rising vapor. Column C1 is operated at total reflux, with the ammonia vapor leaving the top being condensed in the

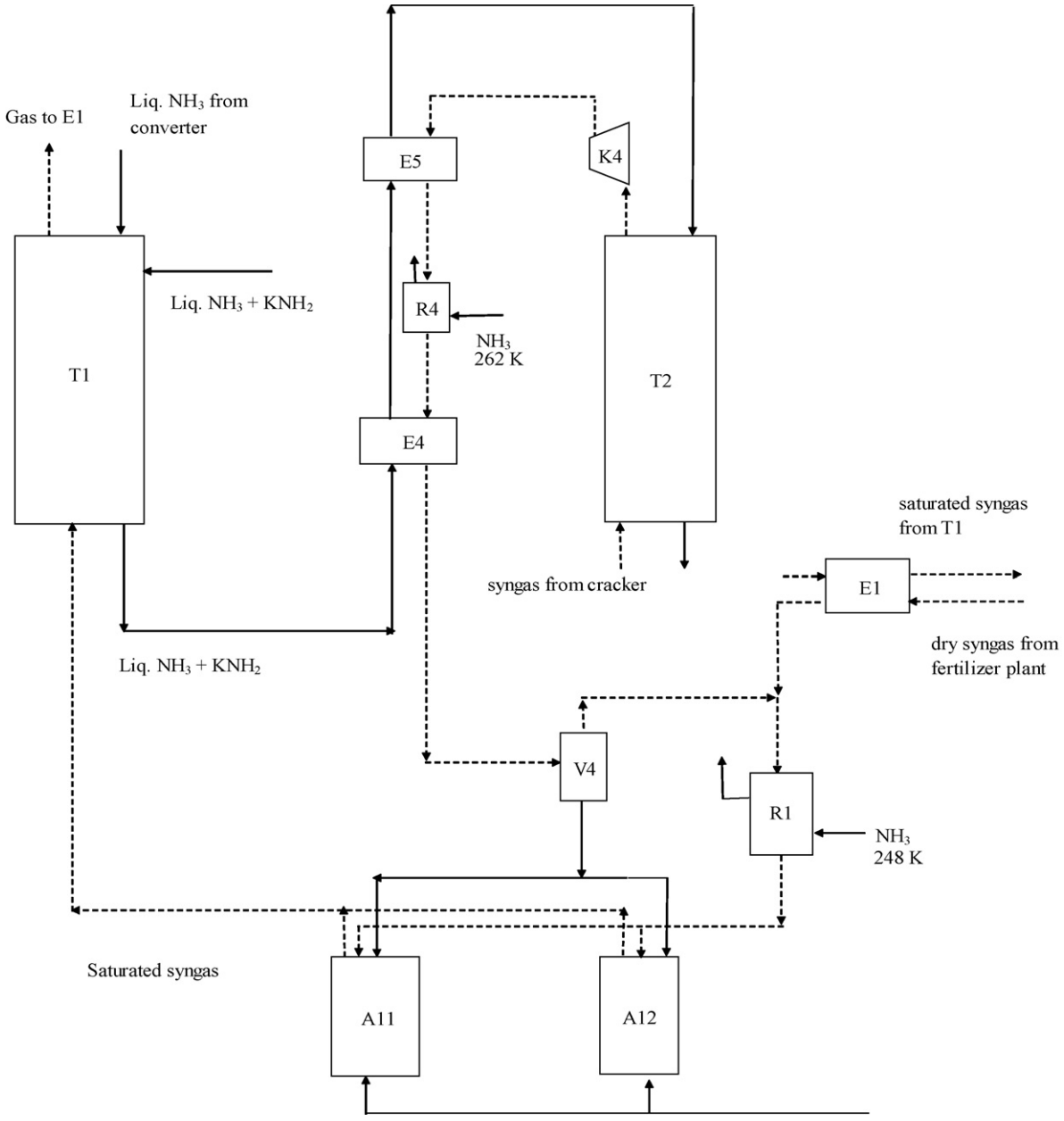

Fig. 3. The heat exchange network between towers T1 and T2.

condensers R1 and R2. Pure liquid ammonia, free from amide is drawn from the middle of the column to vessel V3 and pumped to the cracker.

The deuterium enriched liquid leaving T2 contains the bulk species NH_3, N_2, H_2, KNH_2 and the deuterated species HD and NH_2D. Since, the catalyst gets separated in the vessel C11, the governing equations for N_2, H_2, HD, NH_3 and NH_2D in the column C1 are as follows:Component mass balance

$$L_{i,j-1} + G_{i,j+1} - G_{i,j} - L_{i,j} = 0, \qquad i = 1 \ldots 5 \tag{4}$$

Phase equilibrium relation (considering only bulk components)

$$\frac{G_{i,j}}{\sum_{i=1}^{3} G_{i,j}} = K_{i,\mathrm{ph}} \frac{L_{i,j}}{\sum_{i=1}^{3} L_{i,j}}, \qquad i = 1 \ldots 5 \tag{5}$$

Energy balance

$$\sum_{i=1}^{4} G_{i,j+1} h^{\mathrm{G}}_{i,j+1} + \sum_{i=1}^{4} L_{i,j-1} h^{\mathrm{L}}_{i,j-1} - \sum_{i=1}^{4} G_{i,j} h^{\mathrm{G}}_{i,j} - \sum_{i=1}^{4} L_{i,j} h^{\mathrm{L}}_{i,j} = 0 \tag{6}$$

Phase equilibrium constants

$$K_{i,\mathrm{ph}} = \frac{H_i \gamma_i}{P \varphi_i} \qquad \text{for } H_2,\ \text{HD and } N_2 \text{ as supercritical gases} \tag{7}$$

$$K_{i,\mathrm{ph}} = \frac{P_{\mathrm{sat}} \gamma_i}{P \phi_i} \qquad \text{for } NH_3 \text{ and } NH_2D \text{ as condensable} \tag{8}$$

Chemical equilibrium between HD and NH_2D in the liquid phase according to Eq. (1)

$$K_{\mathrm{eqm}} = \frac{C_{NH_2D} C_{H_2}}{C_{NH_3} C_{H_2}} \tag{9}$$

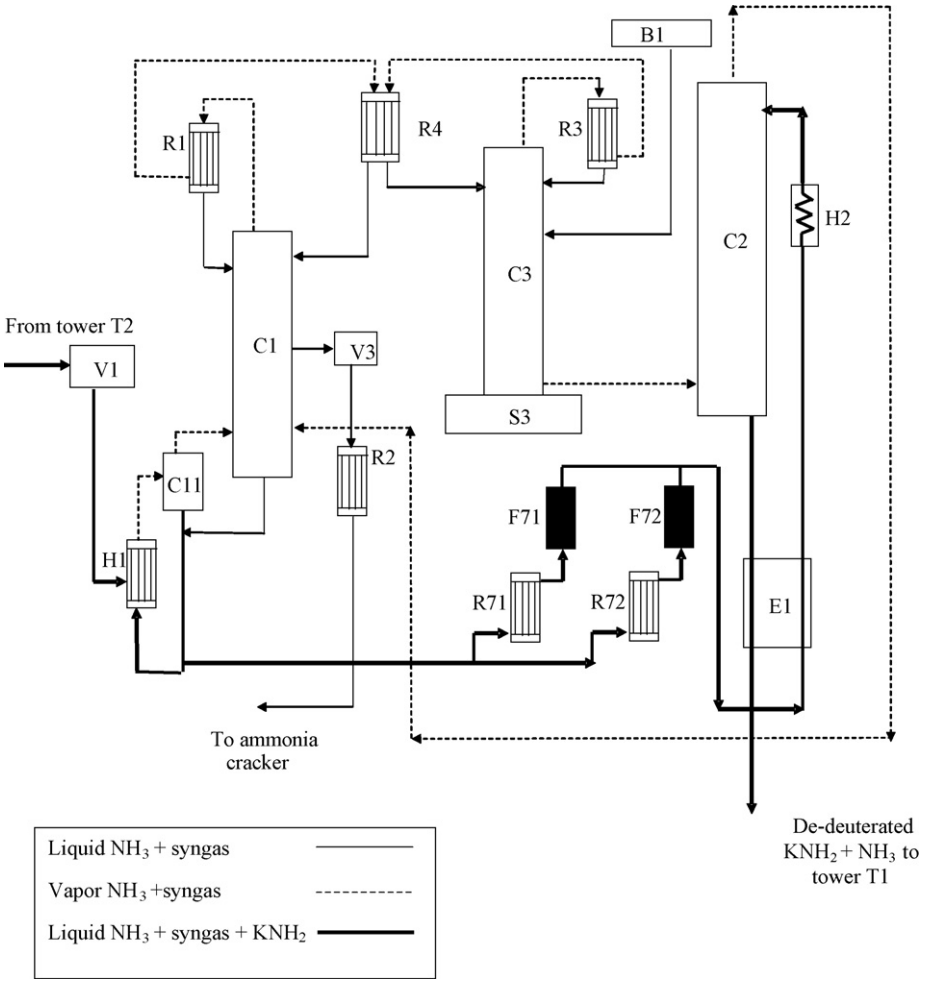

Fig. 4. The catalyst stripping unit.

The following assumptions were made while developing a mathematical model for the distillation column C1:

(1) The liquid and gas streams leaving a particular sieve tray are in thermal and physical equilibrium.
(2) Heat effects of the reactions are neglected.
(3) The phase equilibrium constant for NH_2D is taken to be the same as that of ammonia.
(4) Deuterium stripping from catalyst is complete.

The phase equilibrium for the bulk components, N_2, H_2 and NH_3 at the operating conditions has been modeled by using the $\gamma - \phi$ approach [4]. This model includes the gas phase association of ammonia using a modified Association + Redlich Kwong EOS and represents the liquid phase non-idealities using the NRTL approach [4]. The liquid ammonia concentrated with potassium amide leaving C11 and C1 is still enriched in deuterium and this if recycled directly to the tower T1, can lead to an isotopic bypass increasing the concentration of deuterium in the synthesis gas going out of tower T1. Thus, deuterium is stripped from the concentrated amide solution by contacting it in a counter-current manner with pure ammonia vapors lean in deuterium in the column C2.

The solution coming from C1 is cooled to 268 K in ammonia cooler R71. At this temperature the impurities are precipitated and filtered out in filters F71. The filtered amide solution is pumped through heat exchanger E1 and heated to 333 K in heater H2 by hot water before being fed to the top of the column C2. This column contains a total of 133 trays for mass transfer. Ammonia vapors lean in deuterium vaporized from the storage tank S3 are fed to the bottom of the column C2. The deuterium rich liquid transfers its deuterium to the counter flowing deuterium lean vapor by equilibration on the stages. The depleted liquid leaving the bottom of the column C2 is cooled in E1 and pumped to the exchange tower T1. The vapor ammonia leaving the column C2 at the top enters the column C1 below the washing zone. The deuterium equilibration on the trays represented by Eq. (10)

$$KNHD_{(l)} + NH_{3(g)} \rightarrow KNH_{2(l)} + NH_2D_{(g)} \quad (10)$$

is fairly rapid [1]. The kinetics of the above reaction are not available in the open literature, however, the equilibrium separation factors have been measured by Petersen and Benedict [5]. Thus, a separation factor based approach based on the total deuterium atom fraction D/D + H is followed to evaluate the de-deuteration of the catalyst stream. The separation factor β is represented as a function of operating pressure, P of column C2 and the atom fraction of total deuterium in the liquid X_D [5],

$$\ln \beta = 0.0395 - 0.0128(X_D - 0.424) - 0.01246 \ln(P) \quad (11)$$

where

$$\beta = \frac{[D/D + H]_{Liq}}{[D/D + H]_{Gas}} \quad (12)$$

The isotopic species HD and NH_2D are lumped together as the deuterium atom fraction D/D + H in both the phases. The governing

mass and energy balance equations and assumptions for the bulk species NH_3, N_2 and H_2 in column C2 are similar to that of the column C1.

4. Ammonia vaporization unit

This unit comprises of a column C3 having 13 sieve trays and an ammonia evaporator cum storage vessel S3. The main function of this section is to degas the expanded ammonia and provide the vapor ammonia for the isotopic exchange in C2. The liquid ammonia from the storage vessel B1 is expanded to a low pressure and added to the top of the column C3. The degassed liquid ammonia is collected in S3 and is vaporized using steam. This provides the vapor flow in C2 as well as in C3. Column C3 is also operated at a total reflux, with the ammonia vapor leaving the top being condensed in the condensers R3 and R4.

Since, pure ammonia, lean in deuterium, is simply vaporized in column C3, liquid ammonia along with dissolved nitrogen and hydrogen are the only components present. The governing equations for mass and energy balances and the assumptions over a particular sieve tray are the same as that for the columns C1 and C2.

5. The ammonia synthesis unit

The ammonia synthesis unit is an axial flow four-bed quench type unit, where a hydrogen–nitrogen ($N_2 + 3H_2$) mixture is reacted over the catalyst bed at elevated temperatures and pressures. The reaction is exothermic and temperature in the reactor is sustained by the heat of reaction, a feed-effluent interchanger and using part of the feed as quench streams for intermediate cooling of the reaction mixture.

A detailed study of the ammonia synthesis unit is necessary to determine the effects of process variables upon the converter performance so as to quantify the effects of any operational changes in exchange tower T1 on the ASU. Mathematical models for simulation and optimization studies have been built up by many workers for various types of ammonia synthesis reactors [6–19]. Quench type converters have been modeled earlier by Shah [9] and Kjaer [12]. Shah [9] proposed that his theoretical model be used for off-line optimization to determine the quench flows and converter temperatures. Baddour et al. [10] fitted data from industrial reactors using the Temkin-Pyzhev rate expression and calculated ideal temperature and composition profiles. Annabel [11] modeled a TVA converter and compared their model results with the operating plant data. Their studies revealed that the converter was close to instability at temperatures favoring maximum ammonia production. Kubec et al. [13] developed a model for a radial flow quench type converter. They suggested the use of a model which would be optimized using dynamic programming. The model parameters would be adjusted using current process data. Gaines [14] developed a model for a four-bed quench type ammonia synthesis unit and studied the effects of process variables upon the converter operation based upon a low pressure (15.2 MPa) plant. The resulting data were used to examine practical and easily implemental methods of converter temperature control. Gaines [15] modeled ammonia synthesis loop consists of two parallel quench type converters, compressors, separator, purge and recycled streams. The model is used to determine the effects of synthesis loop variables upon ammonia production. Singh and Saraf [16] modeled and simulated an industrial axial bed ammonia converter having adiabatic catalyst beds with interstage cooling as well as autothermal reactors. Reddy and Husain [17] optimized the parameters with respect to ammonia production rate, fractional hydrogen conversion and gross profitability such as effect of H_2/N_2 ratio, pressure, gas flow rate and inert concentration. Elnashaie et al. [18] have maximized the ammonia conversion by optimizing the temperature profile along the length of the reactor length. Similar optimization studies have also been done by Mansson and Andresen [19] and compared performance with the conventional operation of ammonia synthesis reactors.

The ASU, at the existing plant, consists of four catalyst packed baskets with annular space in between the outer shell and the catalyst baskets and a central riser for the reactant gas flow as shown in Fig. 5. The total feed to the converter is split into two streams. While one stream is fed directly to the heat interchanger placed at the bottom of the pressure shell, the second stream is further split into three quench streams viz. q_1, q_2 and q_3. The fraction of total gas feed routed through the interchanger q_{int} exchanges heat with the hot product gases coming out of the fourth bed. This gas stream further flows upward through the annular space (between the catalyst basket and the pressure shell) and the central riser and enters the first bed where NH_3 and NH_2D are formed according to Eqs. (13) and (14)

$$\frac{1}{2}N_2 + \frac{3}{2}H_2 \Leftrightarrow NH_3 \tag{13}$$

$$\frac{1}{2}N_2 + \frac{1}{2}H_2 + HD \Leftrightarrow NH_2D \tag{14}$$

The reaction is exothermic and the heat of reaction increases the temperature of the gas mixture. The hot product gas at the exit of the first bed is quenched by a fraction of cold feed gas q_1. The first bed is followed by three catalyst beds, each containing a larger quantity of catalyst and two more quench zones. The hot gas out of the fourth bed is cooled on the tube-side of the heat interchanger before leaving the converter zone. This transfer of heat is necessary to bring the cold feed gas (which is routed on the shell-side of the interchanger) to the reaction temperature. The converter catalyst section consists of an outer pressure shell and a catalyst basket. The catalyst basket is coated with insulation to minimize heat transfer from the hot catalyst bed to the feed gas routed through the annulus. An un-insulated riser tube transports gas from the heat interchanger section to the first bed. The transfer of heat to the riser gas is minimal due to a small heat transfer area and because the riser gas has already been heated to near reaction temperature in the interchanger. The mathematical model for the ASU has to include the chemical kinetics and related heat effects of the exothermic ammonia synthesis reaction along with the heat transfer between the catalyst section, annular region and the central riser.

Consider a cross-sectional element of length dz of ASU comprising of the pressure shell, insulated cylindrical catalyst basket, the annular space between the catalyst basket and pressure shell and the un-insulated central riser for transporting the reactant gases to the first bed. As the exothermic ammonia synthesis reaction takes place in the catalytic bed a large quantity of heat is generated, which is transferred to the reactant gas flowing through the central riser and (to some extent) the annular region.

The simplifying assumptions made in developing the model are

(1) The catalyst section is nearly adiabatic and a uniform radial temperature exists.
(2) The temperature of the gas flowing through the catalyst is assumed equal, at each location to the temperature of catalyst particles.
(3) The velocity profile in the bed is uniform since the bed diameter is much larger than the catalyst diameter.

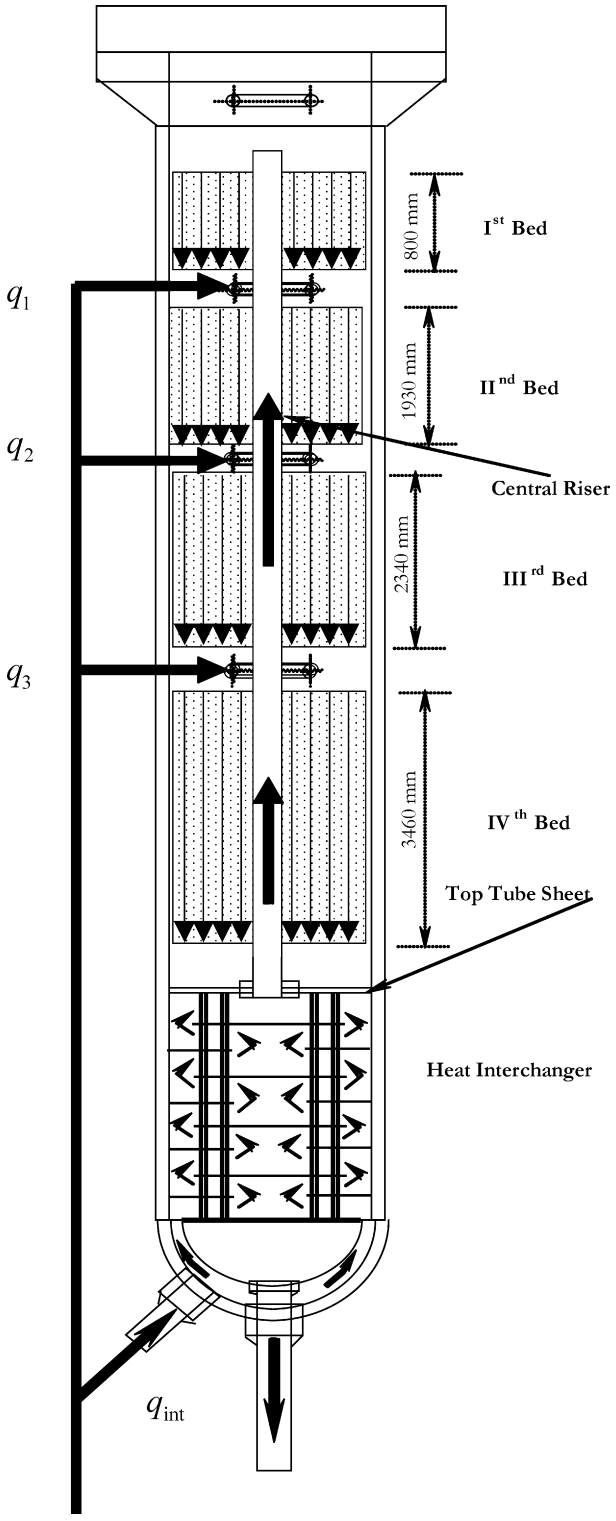

Fig. 5. The ammonia synthesis unit.

The hydrogen material balance on the gas in a differential element of thickness dz of the catalyst bed is given as

$$\frac{d\chi}{dz} = \frac{r_{H_2} A_{bas}}{G^0_{H_2}} \tag{15}$$

The deuterated hydrogen also undergoes synthesis reaction according to Eq. (14). It is assumed that the fraction of H_2 reacted by Eq. (13) is equal to the fraction of HD reacted by Eq. (14). The corresponding molar flows of the respective components inside the bed in terms of the inlet flows can then be written as

$$G_{H_2} = G^0_{H_2}(1-\chi) - \frac{G^0_{HD}\chi}{2} \tag{16}$$

$$G_{N_2} = G^0_{N_2} - \frac{G^0_{H_2}\chi}{3} - \frac{G^0_{HD}\chi}{2} \tag{17}$$

$$G_{NH_3} = G^0_{NH_3} + \frac{2G^0_{H_2}\chi}{3} \tag{18}$$

$$G_{HD} = G^0_{HD}(1-\chi) \tag{19}$$

$$G_{NH_2D} = G^0_{NH_2D} + G^0_{HD}\chi \tag{20}$$

The reaction rate for the reaction represented by Eq. (13) is taken from Dyson and Simons [20] report for the rate of formation of ammonia (kg mol ammonia formed per cubic-meter of catalyst bed per hour)

$$r_{NH_3} = 1.7698 \times 10^{15} \exp\left(\frac{-170397}{RT}\right)\left[K_a^2 a_1 \left(\frac{a_2^{3/2}}{a_3}\right) - \left(\frac{a_3}{a_2^{3/2}}\right)\right] \tag{21}$$

$$r_{H_2} = \frac{3r_{NH_3}\xi\vartheta}{2} = \frac{3r_{NH_3}\Psi}{2} \tag{22}$$

where, R is the universal gas constant 8.314 J/mol K, T is the temperature in K, ξ is the effectiveness factor and ϑ is the catalyst activity. The effectiveness factor and the catalyst activity are lumped together into a single parameter ψ which can be evaluated from the operating plant data of the ammonia converter at the heavy water plant. The terms a_1, a_2 and a_3 are the activities of N_2, H_2 and NH_3, respectively. The equilibrium constant K_a is calculated from the equation of Gillespie and Beattie [15].

$$\log_{10} K_a = -2.691122 \log_{10} T - 5.519265 \times 10^{-5} T + 1.848863 \times 10^{-7} T^2 + \frac{2001.6}{T} + 2.6899 \tag{23}$$

where T is temperature in Kelvin.

The activity of a pure component is given as

$$a_i = P y_i \gamma_i \tag{24}$$

The activity coefficients for nitrogen (1), hydrogen (2) and ammonia (3) are given by the correlations (25), (26) and (27), respectively [15].

$$\gamma_2 = \exp\{e^{(-3.8402T^{0.125}+0.541)P} - e^{(-0.1263T^{0.5}-15.980)P^2} + 300[e^{(-0.011901T-5.941)}](e^{-P/300}-1)\} \tag{25}$$

$$\gamma_1 = 0.93431737 + 0.3101804 \times 10^{-3} T + 0.295896 \times 10^{-3} P - 0.2707279 \times 10^{-6} T^2 + 0.4775207 \times 10^{-6} P^2 \tag{26}$$

$$\gamma_3 = 0.1438996 + 0.2028538 \times 10^{-2} T - 0.4487672 \times 10^{-3} P - 0.1142945 \times 10^{-5} T^2 + 0.2761216 \times 10^{-6} P^2 \tag{27}$$

Heat transferred to the reactant gas flowing in the annulus on the outside of the catalyst basket is computed by

$$G_{ann} C_p \frac{dT_{ann}}{dz} = -\frac{\lambda_{ins}\pi d^o_{bas}(T_{bed} - T_{ann})}{t_{bas}} \tag{28}$$

The catalyst basket insulation is the only major resistance to heat transfer considered, while neglecting the other heat transfer resistances. This reduces the computational effort substantially without affecting the accuracy of the simulation.

The central riser is un-insulated and, therefore, an overall heat transfer coefficient needs to be considered in setting up the energy balance. Thus, the overall heat transfer coefficient U_{ris} for transfer of heat from the catalyst bed to the central riser can be represented as follows,

$$\frac{1}{U_{ris}} = \frac{1}{\hbar_o} + \frac{1}{\hbar_{io}} + \frac{d^o_{ris}}{2\lambda_{ris}\ \ln(d^o_{ris}/d^i_{ris})} \tag{29}$$

The heat transfer coefficient inside packed tubes is evaluated from the correlation reported by Gaines [14].

$$\hbar_o = \frac{19.87\ \exp(-4.6(d_p/d^o_{bas}))(d_p/A_{bas})^{0.7}}{d^o_{bas}} \left(\frac{\lambda}{\mu^{0.7}}\right) W^{0.7} \tag{30}$$

where W is in kg/h, d_p and d^o_{bas} in m, A_{bas} in m^2, λ in W/m K, μ in kmol/m s and $\hbar_o$ in W/m^2 K. The heat transfer coefficient inside the riser is calculated from the Colburn equation [14]

$$\hbar_{io} = 0.1306\dot{m}C_p Pr^{-2/3} Re^{-0.2} \left(\frac{d^i_{ris}}{d^o_{ris}}\right) \tag{31}$$

where $\dot{m}$ is the mass velocity in kmol/s m^2, C_p in kJ/kmol K, $\hbar_{io}$ in W/m^2 K. Thus the heat transferred to the reactant gas flowing through the central riser is given as

$$G_{ris}C_p \frac{dT_{ris}}{dz} = -U_{ris}\pi d^o_{ris}(T_{bed} - T_{ris}) \tag{32}$$

Next, the energy balance for the gas flowing inside the catalyst bed can be written as

$$-G_{bas}C_p \frac{dT_{bed}}{dz} = \frac{2}{3}\Delta H_r r_{H_2} A_{bas} + \frac{\lambda_{ins}\pi d^o_{bas}(T_{bed} - T_{ann})}{t_{bas}} + U_{ris}\pi d^o_{ris}(T_{bed} - T_{ris}) \tag{33}$$

In the above equation, the first term on the RHS is the heat generated by the formation of ammonia, where ΔH_r is in kJ/kmol of ammonia produced. The second and third terms are the heat lost to the annulus and riser, respectively. The heat of reaction (ΔH_r) can be calculated by using the formula of Gillespie and Beattie as described by Strelzoff [21]

$$\Delta H_r = -38225 - 31.23T + 1.54 \times 10^{-2}T^2 - 1.97 \times 10^{-6}T^3 \tag{34}$$

For, the energy balance around the quench zones above each bed, it is assumed that the zones are adiabatic and perfectly mixed. Thus, by equating the energy flow from the previous bed and the energy flow from the quench zone to the energy flow into the next bed for the nth quench zone yields.

$$F_{2n}h(T_{2n}, P) = F_{2n-1}h(T_{2n-1}, P) + q_n G_{feed} h(T_F, P) \tag{35}$$

Similarly, flow out of the quench zone is equal to the sum of the flows entering, since no reaction occurs.

The energy balance for the heat interchanger located at the bottom of the converter is obtained from the heat transfer equations. The cold feed gas flows on the shell-side counter-current to the product gases which is routed through the tube-side. Thus,

$$\frac{dT_S}{dz} = \frac{U_{int}N_{tube}\pi d^o_{tube}(T_S - T_T)}{q_{int}G_{feed}C_P} \tag{36}$$

$$\frac{dT_T}{dz} = \frac{-U_{int}N_{tube}\pi d^o_{tube}(T_S - T_T)}{G_{product}C_P} \tag{37}$$

The overall heat transfer coefficient U_{int} for heat interchanger is calculated from Eq. (29). The shell-side heat transfer coefficient $\hbar_o$ for the heat exchanger is computed by the method of Donohue [14] for disk-and doughnut baffles,

$$\hbar_o = 1.306 d_e^{0.6} Re^{0.6} Pr^{0.33} \tag{38}$$

where d_e is the equivalent diameter is given by

$$d_e = 4\left(\frac{\text{flow area}}{\text{wetted perimeter}}\right) \tag{39}$$

and $\hbar_o$ is in W/m^2 K. The Reynold's number in the above expression is based on S_e, the geometric mean of the cross-flow area and the baffle-hole areas

$$S_e = (\text{cross flow area} \times \text{baffle hole area})^{0.5} \tag{40}$$

and is given as

$$Re = \frac{d^o_{tube}G}{S_e\mu} \tag{41}$$

The individual heat transfer coefficient for the tube-side $\hbar_{io}$ is computed according to Eq. (31).

The model equations cannot be solved analytically because they are highly non-linear and coupled due to heat transfer between the feed and the reacted gas. According to the solution methodology, the riser and annulus temperatures at the top viz. T_{RT} and T_{AT} are assumed. Thus for a given feed gas flow and compositions the conditions at the entry of the first bed are known (see Fig. 6). An integration of Eqs. (15), (28), (32), (33) through the first bed is performed using a fourth order Runge–Kutta method. The conversion with respect to hydrogen (χ) denoted in Eqs. (15)–(18) is set to zero to start the integration. The pressure is assumed to vary linearly with the fraction of the catalyst traversed.

$$P = P_{bot} + \frac{\Delta P(\text{Ht} - z)}{\text{Ht}} \tag{42}$$

and z is the position from the top. The values of $d\chi/dz$, dT_{ann}/dz, dT_{ris}/dz and dT_{bed}/dz for the element are found from Eqs. (15), (28), (32) and (33), respectively, which result into new values for χ, T, T_{ann} and T_{ris} at the end of each integration step.

At the end of integration for a single bed, the compositions are adjusted with reference to the fraction of hydrogen converted according to Eqs. (16)–(20) and the temperature and composition in the next quench zone are computed, which are the initial values for the next bed. This procedure is repeated for each bed till the end of the catalyst section. Next, using the product gas flow and temperature obtained at the end of the fourth bed viz. F_7 and T_7 and the temperature of gas at the bottom of riser and annulus as the initial conditions, the Eqs. (36) and (37) are integrated using Runge–Kutta fourth order method along the length of the interchanger to obtain T_F and T_P. The value of T_F obtained from the interchanger calculation is compared with the known value and accordingly the temperatures T_{RT} and T_{AT} are adjusted and the procedure was repeated.

The model parameter ψ and the quench fractions q_{int}, q_1, q_2 and q_3 are evaluated using the operating plant data of the ASU. A typical operating plant data consists of the total gas feed rate, compositions, T_F, T_P, y_{NH_3} at the entry and exit of each bed and the temperatures T_1–T_7. The values of evaluated parameters and corresponding comparison of model predictions with the operating plant data are shown in Table 2 and Fig. 7. The corresponding temperature and composition profiles along the length of the catalyst bed are shown in Figs. 8 and 9, respectively.

The effect of the synthesis loop variables such as the temperature of feed gas stream and the percentage ammonia in the feed were studied. A base case for the simulation was established as

Table 2
Evaluation of quench fractions and ψ from the operating plant data

		T (K) (plant data)	T (K) (simulated)	% y_{NH_3} plant data	% y_{NH_3} simulated	Operating parameters from simulation
Bed 1	In	643.5	643.5	1.68	1.68	
	Out	786.0	788.4	10.20	10.02	$q_{int} = 0.55$
Bed 2	In	667.5	668.9	7.60	7.67	$q_1 = 0.2$
	Out	781.4	783.6	14.60	14.48	$q_1 = 0.18$
Bed 3	In	679.0	680.7	11.70	11.76	$q_1 = 0.07$
	Out	756.1	754.8	16.20	16.18	$\psi = 0.9$
Bed 4	In	715.6	714.4	14.90	15.04	
	Out	775.1	773.0	18.50	18.5	

shown in Table 3. As discussed elsewhere [14] the temperatures of the first and second beds have little effect on the production as long as they are operated in the feasible operating range. However, the ammonia production may get affected if the third bed temperature is too high. At higher temperature, in the third bed, the reaction rate is decreased as equilibrium conditions are approached. Moreover, the temperature of the outlet gas must be greatly reduced to maintain the fourth bed temperature. Thus, less conversion in the third bed coupled with additional quench substantially reduces the ammonia concentration in the gas entering the fourth bed. The fourth bed temperature is the temperature of greatest consequence,

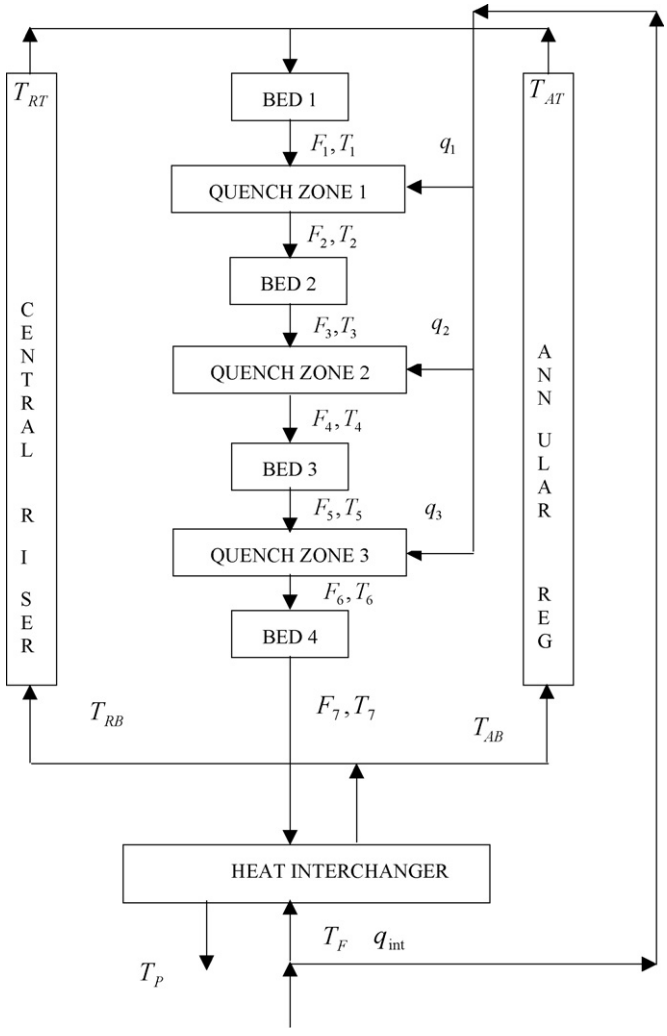

Fig. 6. Block diagram for the mathematical model of the converter.

Table 3
Base case for the study of operating variables on converter performance

Inlet pressure	21.7 MPa
Outlet pressure	21.4 MPa
Feed temperature	428.0 K
H_2 in feed	5291.2 kmol/h
N_2 in feed	1764.0 kmol/h
NH_3 in feed	121.3 kmol/h
Fraction feed through interchanger	0.55
Fraction feed for second bed quench	0.2
Fraction feed for third bed quench	0.18
Fraction feed for fourth bed quench	0.07
Outlet temperature of bed 1	816.6 K
Outlet temperature of bed 2	800.9 K
Outlet temperature of bed 3	772.5 K
Outlet temperature of bed 4	776.6 K
H_2/N_2 ratio	3.0
Mole fraction ammonia in feed	0.0169
Mole fraction ammonia in effluent	0.1924

and the effects of other process variables may be related to this temperature [14]. The variables of concern for the operation of the ammonia converter in the heavy water plant are the temperature of the feed gas to the converter and the ammonia content in the feed to the converter. Initially the quench fractions q_{int} and q_3 were adjusted so as to obtain high converter temperatures. The temper-

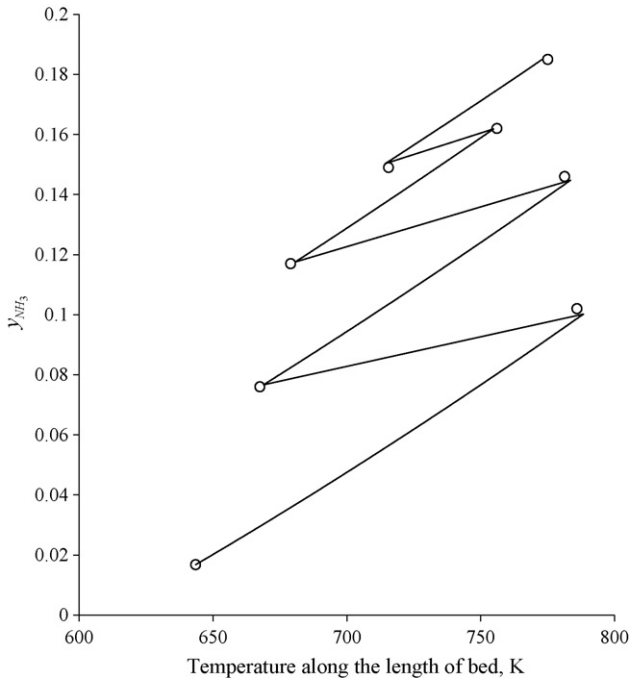

Fig. 7. Simulated temperature profile inside the catalyst tubes with respect to y_{NH_3} and comparison with plant data. (○) Plant data; (—) simulated.

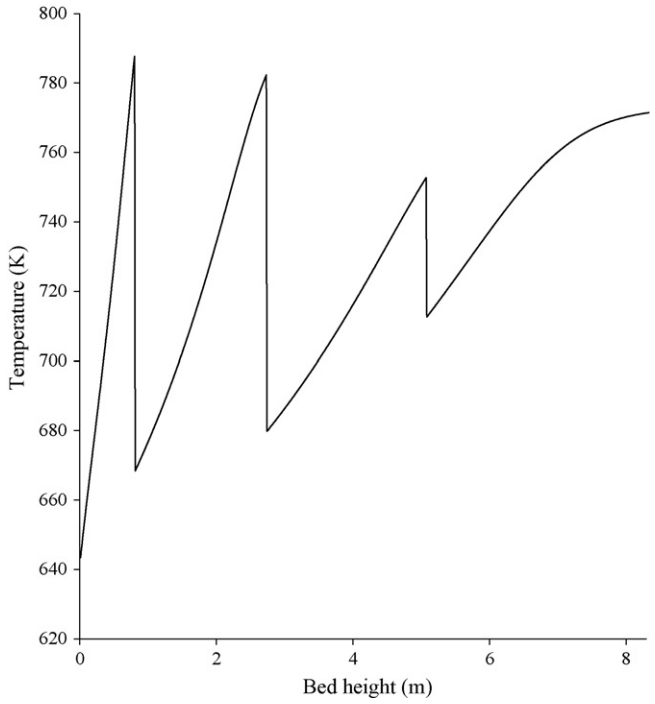

Fig. 8. Temperature profile of gas along the length of catalyst bed.

ature of the fourth bed was then decreased by varying q_3 and q_{int}, while keeping q_1 and q_2 constant and a decreasing temperature profile in the fourth bed was obtained. The fourth bed temperature became increasingly sensitive to the fraction of the feed gas through interchanger (q_{int}) as the operating temperature was reduced. The effect of feed temperature on the converter efficiency is not significant; however, a lower feed temperature gives slightly better conversion as shown in Fig. 10.

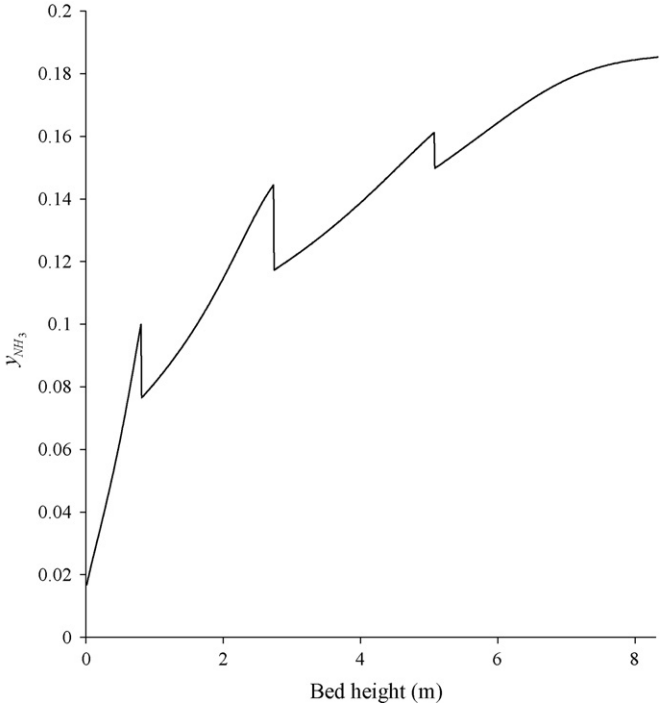

Fig. 9. Composition profile of ammonia along the length of catalyst bed.

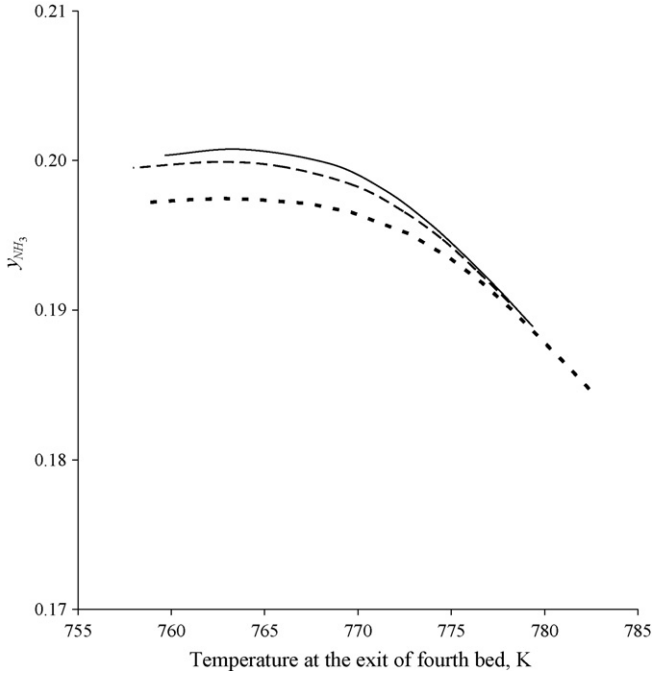

Fig. 10. Effect of temperature on the final conversion. (—) 418 K; (- - -) 428 K; (– – –) 438 K.

The study of the effect of ammonia concentration in the feed on the converter efficiency forms a crucial part of the overall simulation of the Primary Enrichment Section. The converter was simulated at three different feed concentrations of ammonia corresponding to three operating temperatures of the exchange tower T1. Hydrogen and ammonia are the major constituents of gas and liquid phases, respectively. Fig. 11 gives simulated hydrogen and ammonia concentration profiles in the gas and liquid phases of tower T1 for temperatures 248 K, 258 K, 268 K and pressure of 21.7 MPa at the entry of the tower. A feed concentration of 1.69% ammonia in the syngas leaving the exchange tower T1 and entering the converter (after superheating to 428 K) corresponds to the ammonia content in the saturated syngas leaving tower T1 at 253 K and 21.7 MPa. Similarly the feed concentrations, 2.47% and 2.96%, correspond to operating temperatures of 263 K and 268 K, respectively. The % conversion of the syngas to ammonia decreases with the increase in the ammonia concentration in the feed as shown in Fig. 12. The total ammonia content in the syngas leaving ammonia converter is the sum of ammonia in converter feed and ammonia produced by catalytic conversion in the reactor. Ammonia converter's performance is adversely affected by the increase in ammonia content due to reversible nature of reaction. However, simulation shows that the total ammonia content in the product of ammonia converter decreases if ammonia concentration in the feed exceeds 2.96% (Fig. 13). The simulation studies clearly indicate that the exchange tower T1 can be operated at higher temperatures (258–263 K for this particular case) without any adverse effect on the conversion of syngas in ASU.

6. The ammonia cracker

The syngas reboil vapor to the tower T2 is supplied by chemically converting the deuterium rich ammonia, devoid of the catalyst, from the catalyst stripping unit (tower C1) to syngas by the reversible reaction

$$NH_3 \Leftrightarrow \frac{1}{2}N_2 + \frac{3}{2}H_2 \quad (43)$$

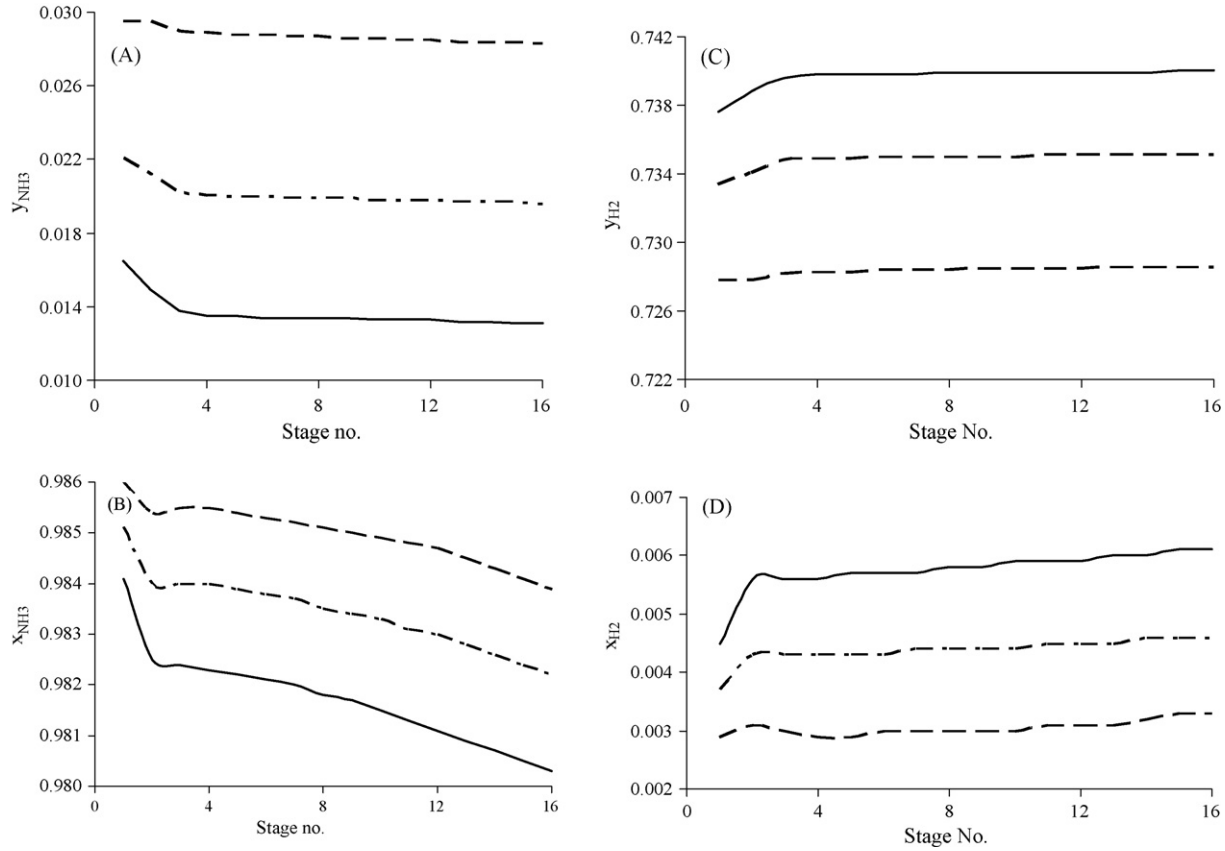

Fig. 11. Simulated composition profiles of H_2, NH_3 of tower T1 at various temperatures. (A) Mole fraction of ammonia in gas phase, (B) mole fraction of ammonia in liquid phase, (C) mole fraction of hydrogen in gas phase, (D) mole fraction of hydrogen in liquid phase. (——) 248 K; (– · – ·) 258; (— —) 268 K.

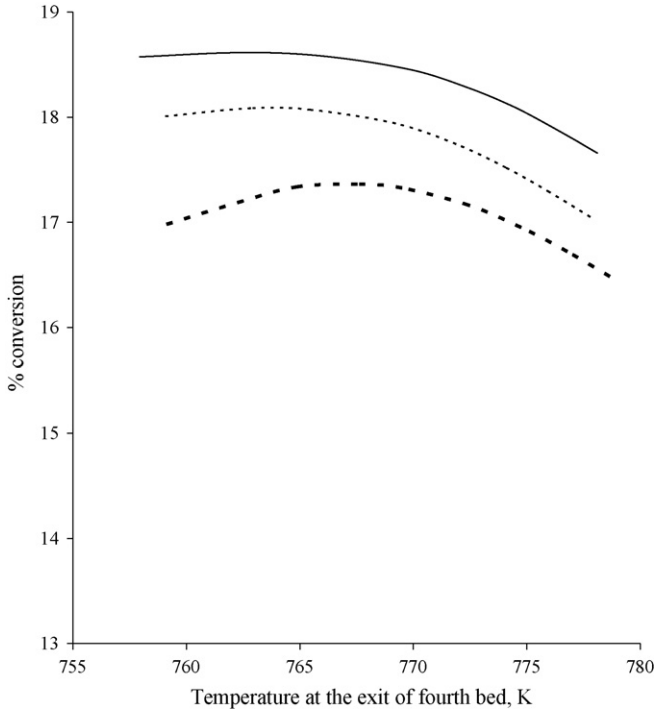

Fig. 12. Effect of feed ammonia concentration on the percentage conversion of syngas to ammonia. (—) 1.69% ammonia in feed; (- - -) 2.57% ammonia in feed; (– – –) 2.96% ammonia in feed.

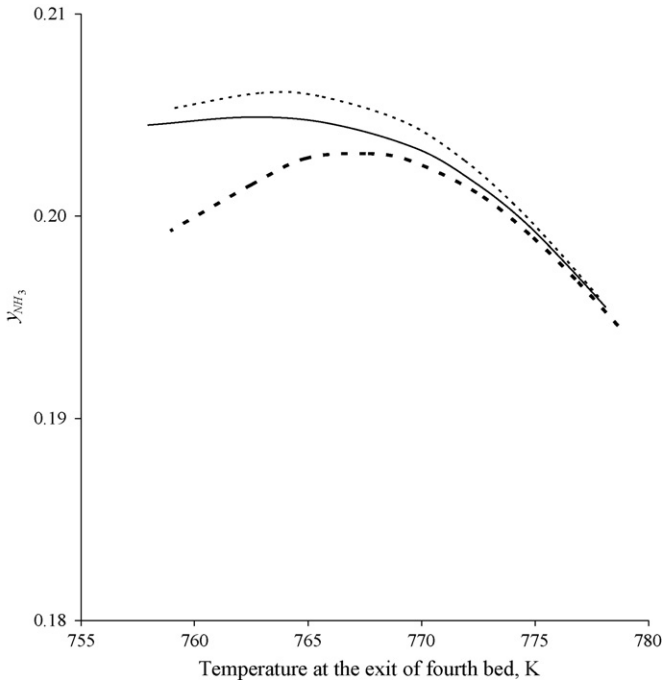

Fig. 13. Effect of feed ammonia concentration on the ammonia content in the product stream. (—) 1.69% ammonia in feed; (- - -) 2.57% ammonia in feed; (– – –) 2.96% ammonia in feed.

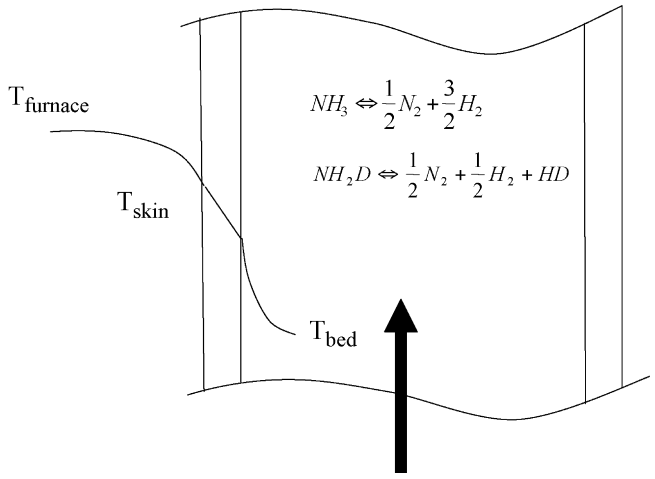

Fig. 14. The heat transfer over a cross-section of a single catalyst tube.

$$NH_2D \Leftrightarrow \frac{1}{2}N_2 + \frac{1}{2}H_2 + HD \quad (44)$$

This reaction is endothermic and, therefore, high temperatures (873–923 K) have to be maintained to sustain the reaction. As in the previous section assumption is made that the conversion χ for both the reactions represented by Eqs. (43) and (44), is the same. The liquid ammonia leaving the distillation tower C1 is preheated to 413 K and the reactant gas is fed directly to the cracker. The cracker consists of a vertical bank of 70 packed tubes of length 12 m each, enclosed inside a gas fired furnace which is maintained at temperatures of around 1173–1213 K necessary for the endothermic reaction.

A mathematical model is developed to simulate the cracker at the heavy water plant, based on the cracker details and design data. A typical cross-section of the cracker tube is shown in Fig. 14. The following mass balance equations can be written for the cross-section of the cracker tube of length dz.

$$\frac{d\chi}{dz} = \frac{-r_{NH_3}A_{cra}}{G^0_{NH_3}} \quad (45)$$

$$G_{H_2} = G^0_{H_2} + \frac{3G^0_{NH_3}\chi}{2} + \frac{G^0_{NH_2D}\chi}{2} \quad (46)$$

$$G_{N_2} = G^0_{N_2} + \frac{G^0_{NH_3}\chi}{2} + \frac{G^0_{NH_2D}\chi}{2} \quad (47)$$

$$G_{NH_3} = G^0_{NH_3}(1-\chi) \quad (48)$$

$$G_{HD} = G^0_{HD} + G^0_{NH_2D}\chi \quad (49)$$

$$G_{NH_2D} = G^0_{NH_2D}(1-\chi) \quad (50)$$

The energy balance for the heat transfer from the furnace walls to the catalyst particles can be written as (Fig. 14)

$$Q = f\pi d^o_{tube} l_{tube} N_t \sigma (T^4_{fur} - T^4_{skin}) = U\pi d^o_{tube} l_{tube} N_t (T_{skin} - T_{bed}) \quad (51)$$

$$\frac{1}{Ud^o_{tube}} = \frac{\ln(d^o_{tube}/d^i_{tube})}{2\lambda} + \frac{1}{\hbar_i d^i_{tube}} \quad (52)$$

$$GC_P \frac{dT_{bed}}{dz} = f\sigma\pi d^o_{tube} N_t (T^4_{fur} - T^4_{skin}) - \Delta H_{rxn} r_{NH_3} A \quad (53)$$

where f is the geometric shape factor for the radiative heat transfer from the walls of the furnace to the catalyst tubes and σ is the Stefan–Boltzman constant. It is assumed that the furnace is maintained at a constant uniform temperature T_f. The shape factor f is determined from the design data for the cracker at the heavy water plant. The cracker is simulated for the design data (as given in Table 4) and the geometric shape factor thus determined was used in subsequent simulation of the PES. The kinetic data for ammonia cracking, specific heats and the transport properties are evaluated from expressions already presented in the previous section.

Table 4
Design data for ammonia cracker

Inlet pressure	14.71 MPa
Outlet pressure	13.2 MPa
Feed temperature	413.0 K
H_2 in feed	2.036 kmol/h
N_2 in feed	4.998 kmol/h
NH_3 in feed	918.64 kmol/h
Temperature at the exit	890.5 K
Average Furnace temperature	1213 K
Mole fraction ammonia in effluent	0.059
Value of shape factor f from simulation	0.53

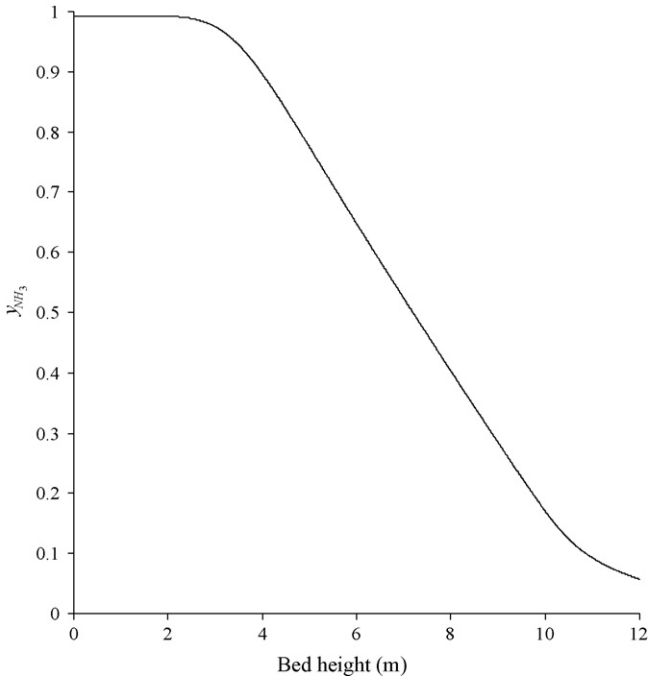

Fig. 15. Composition profile of ammonia along the length of cracker.

The composition and temperature profiles in the catalyst tubes are shown in Figs. 15 and 16, respectively. The conversion of ammonia to syngas is minimal for a length of approximately 2.5 m from the bottom. The feed gas (at a temperature of 413 K) at the point of entry in the cracker has to be heated to a temperature at which the reaction is initiated (~550 K). Thus, the temperature profiles for both the skin temperature and the bed temperature indicate a steep slope during the first 2.5 m of the tube length, which is used to preheat the feed gas with practically no reaction. However, as soon as the reaction starts, (beyond 2.5 m and up to 11.0 m) the slope decreases due to the heat of reaction required for the endothermic reaction. Beyond a tube length of approximately 11 m the rate of the reversible reaction is restricted to some extent due to increasing concentration of the reaction products and therefore, the slope increases towards the end.

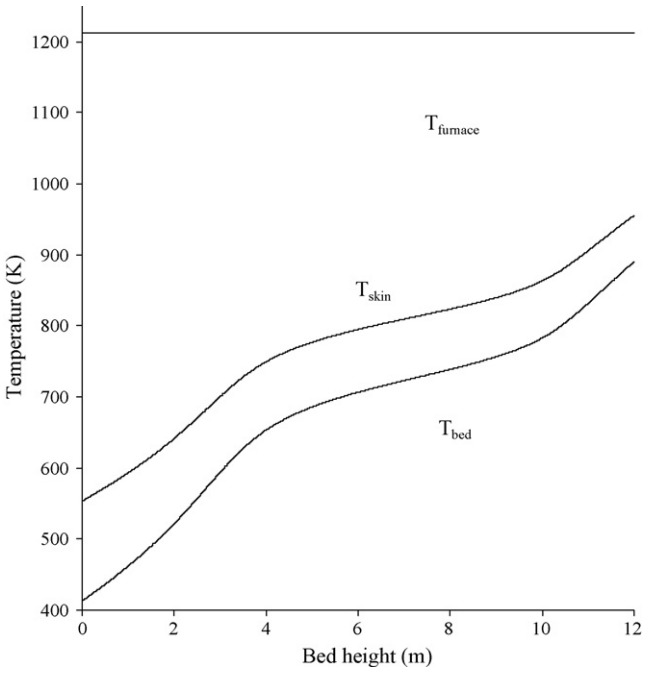

Fig. 16. Temperature profiles in the cracker.

7. Simulation of the overall Primary Enrichment Section flow sheet

The mathematical model for the chemical exchange towers T1 and T2 has been developed in our previous work [3] and the same is being used in the present simulation. The scheme of solution for the entire flow sheet of the Primary Enrichment Section (PES) is shown in Fig. 17. The underlying mass and energy balance equations constituting the unit operations in the flow sheet are simulated based on the method of successive iteration. The iteration procedure starts with the exchange tower T1 which requires an input of temperature and pressure at the bottom of exchange towers, T1 and T2. The other inputs, such as liquid ammonia flow from converter (stream S_1), catalyst solution ($KNH_2 + NH_3$) from the distillation column C2 (stream S_2) and the syngas flow from exchange tower T2 is initialized and the exchange tower T1 is simulated. The exchange tower T2 is simulated next, using the information of the liquid stream leaving T1 and initializing the gas flow from cracker thereby evaluating the stream S_4.

Next, using the output gas stream from the exchange tower T1, the ammonia converter is simulated and the corresponding stream S_1 is updated. This is followed by simulation of the distillation column C3. Using the resulting information and initializing the input stream S_3, the distillation column C2 is simulated. The output streams from the simulation of C2 combined with S_4 evaluated earlier are used as inputs for simulating the distillation column C1, thereby updating the corresponding output stream S_3.

Table 5
Base case for simulating the effect of operating variables on the throughput of NH_2D from PES

Operating temperature of T1 (K)	248
Operating pressure of T1 (MPa)	21.7
Dry syngas from fertilizer plant, TPH	48
Operating temperature of T2 (K)	284
Operating pressure of T2 (MPa)	10.5
Catalyst concentration (g KNH_2/kg NH_3)	25
Conversion of liquid ammonia in cracker (%)	83.5

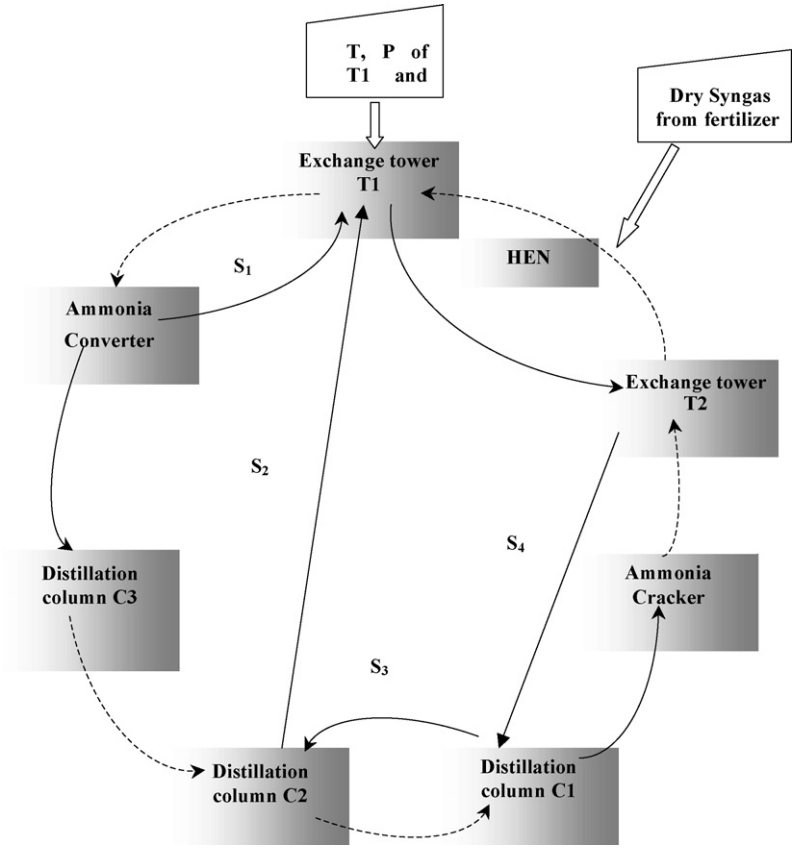

Fig. 17. Information flow diagram for the simulation of the PES. (▭) Input data; (—) liquid stream; (- - -) gas stream.

Table 6
Effect of the operating temperature of T1 on throughput of NH_2D and the coolant requirement in HEN

Operating temperature of T1 (K)	Exit gas D/D + H	kmol NH_2D/h leaving T2	Converter efficiency (%)	Ammonia flow to T1 from converter (kg/h)	Total coolant flow to the condensers R1 + R4 (kg/h)
248	32.18	24.76	18.57	11862	2700
253	23.97	26.09	18.44	11759	2087
256	19.35	26.35	18.36	11677	1615
258	16.83	26.55	18.21	11552	1380
260	14.69	24.75	18.07	11438	1070
263	12.18	23.36	17.8	11218	635

The simulation of column C1 is followed by simulation of ammonia cracker and the simultaneous simulation of the exchange tower T2, which updates the output gas stream from T2. The simulations are repeated and with successive iterations the corresponding composition and temperature profiles get updated and reach a steady state (with respect to the numerical values) at which point the flow sheet is considered to be converged.

8. Effect of the operating temperature of exchange tower T1 on the throughput of NH_2D from the PES

The earlier work on the PIEU of the mono-thermal chemical exchange process predicted that a higher temperature of operation of the exchange tower T1 maximizes the extraction of deuterium from the syngas [3]. However, a high temperature operation of the tower T1 implies a higher percentage of ammonia in the syngas leaving T1. The gas leaving at the top of the exchange tower T1 constitutes the feed to the ammonia converter which is responsible for providing the liquid ammonia reflux by the chemical conversion of syngas to ammonia. A higher content of ammonia (i.e. product) in the feed to the converter would affect the converter performance adversely, due to increased reversibility of the synthesis reaction (Eq. (13)).

Thus, the overall simulation of the PES flow sheet is performed at different operating temperatures of the exchange tower T1 to assess the overall effect on the final throughput, i.e. the flow rate of the deuterated ammonia (NH_2D) in the enriched liquid ammonia leaving exchange tower T2. A high temperature operation of T1 implies the requirement of additional ammonia in the humidification unit (A11). This is procured by operating the exchange tower T2 at high temperatures. Thus a high temperature of operation of the exchange tower T2 would humidify the resulting gas coming out of the exchange tower T2 to an extent determined by the quantity of ammonia required for humidifying the total syngas stream entering exchange tower T1.

A high temperature operation of the exchange towers T1 and T2 would imply a lesser requirement of the coolant in the heat exchange network between T1 and T2. Thus it would serve a beneficial approach, first in terms of increased productivity and second in terms of reduced operating costs. Subsequently, a base case was established as given in Table 5 and respective cases corresponding to an increased operating temperature of the exchange towers T1 and T2 were simulated, keeping the other operating variables constant. Table 6 shows the results obtained from, the PES simulations at different temperatures.

A higher temperature of operation of column T1 increases the extraction of deuterium in the tower T1 (the exit gas D/D + H concentration of T1 at 263 K reduces by 62.1% with respect to the base case, i.e. 248 K). However, the throughput of NH_2D (kmol per hour) in the liquid stream leaving the exchange tower T2 goes through a maximum at 258 K (increases by 7% from 248 K to 258 K). This is due to the adverse effect of the increasing concentration of ammonia in the syngas stream at high temperatures on the efficiency of the ammonia converter. As can be seen from Table 6, the converter efficiency decreases by 4.1% from 248 K to 263 K and the flow rate of ammonia sent as reflux to T1 decreases by 5.4% from 248 K to 263 K for the case corresponding to an operating temperature of 263 K. However, at the same time a higher temperature of operation reduces the quantity of refrigerant ammonia required in the condensers R1 and R4 (decreases by 49% from 248 K to 258 K) in the HEN between T1 and T2. Thus for the selected base case, increasing the operating temperature from 248 K to 258 K increases the productivity in terms of kmol NH_2D per hour in the enriched liquid stream leaving T2 by *7%* as well as reduces the operating costs in terms of the coolant requirement in the HEN by almost *50%*.

9. Effect of catalyst concentration on the throughput of NH_2D from the PES

In our earlier studies, the mathematical model of the PIEU predicted that an increased catalyst concentration (KNH_2) increases the extraction of deuterium [3]. Thus the effect of the operating temperature of exchange towers T1 (and consequently T2) at different catalyst concentrations is studied by simulating the entire PES flow sheet at the base condition (Table 5).

At a low catalyst concentration of 7.5 g KNH_2/kg NH_3, the rise in productivity is the sharpest from 248 K to 253 K, whereas the corresponding slope of productivity with respect to the operating temperature progressively decreases when the PES is operated at higher catalyst concentrations (Fig. 18). The effect of temperature

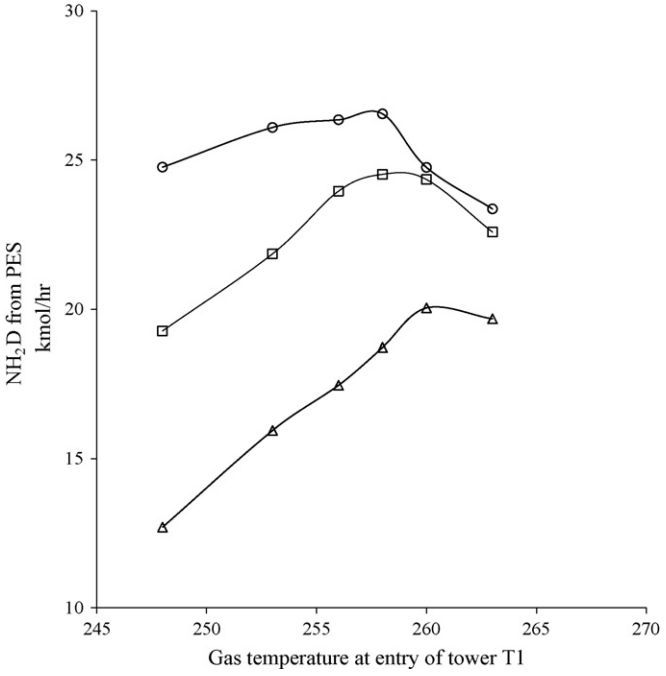

Fig. 18. Effect of the catalyst concentration on throughput of NH_2D. (△) 7.5 g KNH_2/l; (□) 15 g KNH_2/l; (○) 25 g KNH_2/l.

Table 7
Effect of the operating pressure of the exchange tower T1 on the performance of PES

Operating pressure (MPa)	Converter efficiency (%)	kmol NH_2D/h leaving T2	D/D + H gas at exit of T1	Tower L/G (kg/kg)	D/D + H gas at entry to T2	D/D + H gas at exit of T2
21.7	18.58	25.39	32.7	0.2377	9562.3	132.6
19.7	17.04	20.07	32.16	0.2165	8933.9	112.4
17.7	14.54	11.09	34.00	0.1822	6587.6	116.7
16.8	13.4	10.31	35.78	0.1638	7194.9	139.7

on reaction kinetics is more at the lower catalyst concentrations. The optimum temperature range lies between 260 K and 263 K for catalyst concentration of 7.5 g KNH_2/kg NH_3. The optimum temperature (range) decreases as catalyst concentration is increased. The optimum temperature range of 258–260 K for 15 g KNH_2/kg NH_3 decreases further to an optimum operating temperature of 258 K for 25 g KNH_2/kg NH_3.

10. Effect of operating pressure of exchange tower T1 on performance of the PES

The tendency in high pressure processes such as ammonia synthesis is clearly in the direction of lower pressures as new and more efficient catalyst are developed. This, development of new catalysts with increased activity would lower the operating pressure required for the ammonia synthesis.

The heavy water plants based on the mono-thermal ammonia hydrogen exchange process are parasitic to fertilizer plants which supply the deuterium rich syngas ($N_2 + 3H_2$). Thus, a shift from the present day catalysts to modern-day catalysts with higher activity (in the fertilizer plants) would mean a lower operating pressure for ammonia synthesis in these units, thereby resulting in low pressure syngas made available to the heavy water plants. Thus, taking into consideration the future development of the ammonia synthesis catalysts resulting in a shift to low pressure operation, the entire PES was also simulated at low operating pressures.

The base case is again kept constant (Table 5) for all the simulations. The gas leaving the exchange tower T1 is fed directly (after preheating) to the converter at the exit pressure of T1. Thus, a lower operating pressure of exchange tower T1 consequently results in a low pressure operation of the converter. As expected, the converter performance gets affected drastically because of the lower partial pressures of the resulting components. Moreover, for the same gas load, a reduction in the operating pressure reduces the density of the gas mixture, due to which the volumetric gas flow rate increases which in turn results in a lower residence time for the gas through the converter. Both these effects reduce the converter efficiency by 28% when the operating pressure is decreased from 21.7 MPa to 16.7 MPa. These results in a lower flow rate of liquid ammonia reflux to the exchange tower T1 and, therefore, decrease the tower L/G ratio (Table 7). The decrease in the flow rate of liquid ammonia causes the throughput of NH_2D to drop accordingly.

The drastic reduction in the converter efficiency can be avoided by simply changing the existing catalyst with an improved variant (in terms of catalyst activity) or installing additional booster compressors to compress the low pressure syngas from the fertilizer unit.

11. Conclusion

A model of the PIEU of the mono-thermal ammonia hydrogen chemical exchange process is extended to include the Primary Enrichment Section of comprising of the ammonia synthesis unit, the catalyst stripping unit, the ammonia cracker and the heat exchange network between exchange towers, T1 and T2. The PIEU model simulation had predicted that a high temperature operation would be beneficial in terms of increased deuterium extraction. However, it would be limited by the adverse effect on the ammonia synthesis unit. Thus the entire Primary Enrichment Section flow sheet is simulated to quantify the effect of the operating variables on the throughput of NH_2D from the PES. The model predicts that, by changing the operating temperature of the PES from 248 K to 258 K would not only reduce the energy requirement in the HEN by 50% (due to lower refrigerant requirement) but also increases the productivity of heavy water by 7%.

Acknowledgement

The authors acknowledge the financial support extended by the Department of Atomic Energy, Govt. of. India.

References

[1] S.M. Dave, H.K. Sadhukhan, O.A. Novaro, Heavy Water Properties Production and Analysis, Quest Publications, Mumbai, 1997.
[2] M. Benedict, T.H. Pigford, H.W. Levi, Nuclear Chemical Engineering, McGraw-Hill Book Company, New York, 1981.
[3] M.R. Sawant, A.W. Patwardhan, V.G. Gaikar, Simulation of the mono-thermal ammonia hydrogen chemical exchange tower as reactive absorption system, Ind. Eng. Chem. Res. 45 (20) (2006) 6745.
[4] M.R. Sawant, A.W. Patwardhan, V.G. Gaikar, M. Bhaskaran, Phase equilibria analysis of the binary N_2-NH_3 and H_2-NH_3 systems and prediction of ternary phase equilibria, Fluid Phase Equilibria 239 (1) (2006) 52.
[5] G.T. Petersen, M. Benedict, Enrichment of deuterium during distillation, Nucl. Sci. Eng. 15 (1963) 90.
[6] C.V. Heerden, Autothermic processes, Ind. Eng. Chem. 45 (1953) 1242.
[7] J.J. Hay, I.M. Pallai, Calculation problems of ammonia synthesis converters, Br. Chem. Eng. 8 (1963) 171.
[8] P.L.T. Brian, R.M. Baddour, J.P. Eyemery, Transient behaviour of an ammonia synthesis reactor, Chem. Eng. Sci. 20 (1965) 297.
[9] M.J. Shah, Control simulation in ammonia production, Ind. Eng. Chem. 59 (1967) 72.
[10] R.F. Baddour, P.L.T. Brian, B.A. Logeais, J.P. Eymery, Steady-state simulation of an ammonia synthesis converter, Chem. Eng. Sci. 20 (1965) 281.
[11] D. Annabel, Application of the Temkin kinetic equation to ammonia synthesis in large-scale reactors, Chem. Eng. Sci. 1 (1952) 145.
[12] J. Kjaer, Calculation of Ammonia Converters on an Electronic Digital Computer, Akademisk Forlag, Copenhagen, 1968.
[13] J. Kubec, J. Burianova, Z. Burianec, Large ammonia converter designed by the Kralovopolske Strojirny of BRNO, Int. Chem. Eng. 14 (1974) 629.
[14] L.D. Gaines, Optimal temperatures for ammonia synthesis converters, Ind. Eng. Chem. Process Des. Dev. 16 (1977) 381.
[15] L.D. Gaines, Ammonia synthesis loop variables investigated by steady-state simulation, Chem. Eng. Sci. 34 (1979) 37.
[16] C.P.P. Singh, D.N. Saraf, Simulation of ammonia synthesis reactors, Ind. Eng. Chem. Process Des. Dev. 18 (1979) 364.
[17] K.V. Reddy, A. Husain, Modeling and simulation of an ammonia synthesis loop, Ind. Eng. Chem. Process Des. Dev. 21 (1982) 359.
[18] S.S. Elnashaie, A.T. Mahfouz, S.S. Elshishini, Digital simulation of an industrial ammonia reactor, Chem. Eng. Process 23 (3) (1988) 165.
[19] M. Mansson, B. Andresen, Optimal temperature profile for an ammonia reactor, Ind. Eng. Chem. Process Des. Dev. 25 (1986) 59.
[20] D.C. Dyson, J.M. Simon, A Kinetic expression with diffusion correction for ammonia synthesis on industrial catalyst, Ind. Eng. Chem. Fund. 7 (1968) 605.
[21] S. Strelzoff, Technology and Manufacture of Ammonia, Wiley, New York, 1981.